

Strain-induced magnetic anisotropy via the Jahn-Teller effect and the magnetoelastic coupling of tetragonally distorted (Cu,Co)Fe₂O₄ particles

Hawa Latiff^{1,2}, Mikio Kishimoto¹, Jun-ichiro Inoue¹, Eiji Kita¹, Hideto Yanagihara¹, and Thibaut Devillers²

Department of Applied Physics, University of Tsukuba, Tsukuba, Ibaraki 305-8573, Japan
Univ. Grenoble Alpes, CNRS, Grenoble INP, Institut Néel, 38000 Grenoble, France

Abstract—We investigated on the strain-induced magnetic anisotropy via the Jahn-Teller (JT) distortion of Cu²⁺ ions and the magnetoelastic coupling of Co²⁺ ions in Cu_{1-x}Co_xFe₂O₄ particles. The ideal composition for the tetragonalization of (Cu,Co)Fe₂O₄ is confirmed for x in the range of $0 < x < 0.15$. The tetragonally distorted spinel structured (Cu,Co)Fe₂O₄ particles indicate tetragonal distortion of up to 5.6% as a consequence of the JT effect, and increasing the Co content suppressed the cooperative JT distortion. In-field Mössbauer study revealed a 10 % Fe-rich B site due to the anti-site defects. The saturation magnetization increases with x and varies from 26.9 to 36.8 Am²/kg. The coercivity ranges from 68 to 175 kA/m and showed a maximum at $x = 0.1$. The maximum anisotropy field, H_k estimated from torque measurement is 1590 kA/m (20 kOe), with the magnetic anisotropy constant $K = 0.14$ M J/m³. The maximum values of H_c and H_k are explained by the mechanism of magnetic anisotropy from both the lattice distortion of Cu²⁺ and the anisotropy sites of Co²⁺. We showed that the magnetoelastic theory is applicable qualitatively to explain the large anisotropy obtained in the tetragonally distorted particles.

Keywords—spinel ferrite, Jahn-Teller effect, magnetoelastic effect, magnetic anisotropy, coercivity

Introduction

High-performance permanent magnets are among the key components that hold a possible answer to efficient energy conversion technologies. These materials require high curie temperature, high room temperature magnetization, and high coercivity (high magnetic anisotropy). Ferrites are chemically stable and are mostly ferrimagnetic with relatively high saturation magnetization. The anisotropic hexagonal ferrite (Ba- and/or Sr- ferrite) are used commonly as ferrite magnets compared to the cubic type spinel ferrite due to their high magnetic anisotropy field, H_k which may reach up to 995–1400 kA/m ($H_k = 12.5$ – 17.6 kOe). [1]·[2]·[3]·[4] Recent studies showed that high magnetic anisotropy can also be realized in the cubic spinel ferrite by introducing tetragonal distortion in the symmetry. [5]·[6] Niizeki *et al.* reported large perpendicular magnetic anisotropy of over 1.0 MJ/m³ ($H_k \sim 50$ kOe) in the tetragonally strained Co ferrite thin films. The relationship between lattice strain and the uniaxial anisotropy was discussed within the magnetoelastic theory. [7]·[8] It was shown that the magnetoelastic theory is applicable even under a maximum strain of 3%. [9]

For bulk application, the development of tetragonally distorted spinel ferrite in the form of nanoparticles is essential.[10]·[11] We proposed the introduction of a spontaneous lattice strain via the Jahn-Teller (JT) effect of Cu²⁺ ion in (Cu,Co)Fe₂O₄ particles[12] and found that the coercivities were highly dependent to the lattice distortion, similar to previous reports. [13]·[14]·[15] We attributed the high coercivity to the enhanced magnetic anisotropy of the octahedral Co²⁺ ions due to the lattice distortion by the Cu²⁺ ions. Meanwhile,

Villette *et al.* reported on mixed cobalt-copper ferrites acicular particles, where the strain-dependent coercivities were attributed to a combination of structural anisotropy, directional ordering and the acicular shape anisotropy of the particles. Directional ordering[16] of octahedral Co^{2+} and the anisotropy of bulk CoFe_2O_4 has been explained by Slonczewski[17] whereas the model of magnetic shape anisotropy has also been well established[18]. However, the mechanism of strain-induced anisotropy (structural anisotropy) in nanoparticles is still unclarified due many issues including the difficulty in determining the magnetic anisotropy of the randomly-oriented magnetic powders.

In this paper, we propose a physical model of the magnetic anisotropy of the tetragonally distorted $(\text{Cu},\text{Co})\text{Fe}_2\text{O}_4$ particles using a simple phenomenological expression that couples the JT effect and the magnetoelastic effect. For this purpose, we investigated the effect of Co content on the lattice strain and the magnetic anisotropy of the tetragonally distorted $\text{Cu}_{1-x}\text{Co}_x\text{Fe}_2\text{O}_4$ particles. We aim to maximize the magnetic anisotropy by optimizing the amount of Cu and Co to obtain lattice distortion, and activate the magnetoelasticity of Co. The most important point here is to relate the lattice distortion with the magnetic anisotropy (in our case, determined by the rotational hysteresis analysis) rather than with the coercivity. It is also important that we eliminate the shape anisotropy factor to focus exclusively on the strain-induced anisotropy.

Experimental

To eliminate the shape anisotropy factor, we prepared somewhat sphere-like particles (confirmed by the transmission electron microscopy[11][12]). The $\text{Cu}_x\text{Co}_{1-x}\text{Fe}_2\text{O}_4$ particles were synthesized by the coprecipitation and flux treatment methods followed by a heat-treatment process as described in Ref. [11]. The Co content is varied as $x = 0 - 0.2$. The x-ray diffraction (XRD) patterns of the heat-treated $\text{Cu}_{1-x}\text{Co}_x\text{Fe}_2\text{O}_4$ samples showed distinct tetragonal distortions in the $x = 0-0.1$ samples (Figure 1 (a)). Asymmetrical cubic peaks observed for the $x = 0.15$ sample suggests a mixed phase of the cubic and tetragonally distorted spinel structure. Symmetrical cubic peaks observed when $x = 0.2$ indicates the absence of a cooperative JT distortion. The degree of lattice strain, c/a is calculated from the interplanar spacings and lattice constants evaluated from the (004) and the (220) reflections around $41 < 2\theta \text{ (deg.)} < 44$. The tetragonality, defined as $\chi = c/a - 1$ (%), decreases with x due to the suppression of cooperative JT distortion with the decrease in Cu content (Figure 1 (b)). The TEM image reveals spherical particles with diameter of 50 – 100 nm.

Results and Discussion

The crystal structures of CuFe_2O_4 and CoFe_2O_4 are mainly that of an inverse spinel with the cations distribution of $[\text{Fe}^{3+}]_A[M^{2+}, \text{Fe}^{3+}]_B\text{O}_4$. The divalent cations ($M^{2+} = \text{Co}^{2+}, \text{Cu}^{2+}$) are distributed in the octahedral B sublattice and Fe cations evenly distributed in both the tetrahedral A and octahedral B sublattices. Depending on the synthesis methods, anti-site defects may develop, where the divalent ions in the B site interchange with the Fe ions in the A site. Particularly for CuFe_2O_4 , it is crucial that more than 75% of Cu^{2+} ions occupy the B sublattice to exhibit the JT effect. [19][20]

To estimate the amount of anti-site defects, we determined the Fe^{3+} site distribution via the in-field ^{57}Fe Mössbauer experiments at room temperature. Figure 2 shows the zero-field (top) and high-field (bottom) Mössbauer spectra for the tetragonally distorted $\text{Cu}_{0.9}\text{Co}_{0.1}\text{Fe}_2\text{O}_4$ sample. The spectra was fitted using the program MossWin Ver. 4 [21] with the velocity and isomer shift calibrated relative to α -Fe foil. The fitting parameters are listed in Table 1.

The zero-field spectrum indicates almost overlapping two resonance lines, attributed to the A and B sublattices. By applying an external field B_{ext} along the γ -ray incident direction, we observed the disappearance of the $\Delta m = 0$ lines, showing the collinearity of the Fe (A) and Fe (B) moments with the field.[22] The direction of B_{ext} always opposes the direction of the internal (hyperfine) field B_{hf} due to the s-d coupling of the electrons at the nuclei. In antiferromagnetic/ferrimagnetic materials where two or more internal field directions are present, we can distinguish the sublattice resonance lines from the opposite effects of the applied field. In our sample, the B_{hf} measured at zero field are; $B_{\text{hf}}(\text{A}) = 47.99 (\pm 0.03)$ T and $B_{\text{hf}}(\text{B}) = 50.84 (\pm 0.03)$ T. At high field, the B_{hf} caused by the majority spin (B-site) decreased by 5 T to 46.27 (± 0.03) T, whereas that caused by the minority spin (A-site) increased by 5 T to 53.10 (± 0.03) T. This result is consistent with the Néel[23] model of antiferromagnetically coupled collinear A and B sublattices. Furthermore, by deducting the $B_{\text{ext}} = 5$ T contribution, the obtained B_{hf} values are in agreement with the zero-field literature values for tetragonal copper ferrite which are $B_{\text{hf}}(\text{A}) = 48.6 (\pm 0.3)$ T and $B_{\text{hf}}(\text{B}) = 50.7 (\pm 0.3)$ T. [24]

Since the population area (%) of Fe(A) and Fe(B) are determined from the integrals of each resonance lines, the large margin of error in the line widths of the zero-field spectrum make the calculation highly unreliable. Applying an external field helps to resolve the resonance lines and thus giving a higher accuracy of the fitting parameters. From the high-field fitting parameters, the cation distribution is estimated as $[(\text{Cu},\text{Co})^{2+}_{0.13}\text{Fe}^{3+}_{0.87}]_{\text{A}}[(\text{Cu},\text{Co})^{2+}_{0.87}\text{Fe}^{3+}_{1.13}]_{\text{B}}\text{O}_4$. Our sample contained 13% of anti-site defects which are considered negligible to the JT distortion.

Figure 3 shows the variation of saturation magnetization M_s and coercivity H_c measured using a vibrating sample magnetometer (VSM) at room temperature under a maximum applied field of 1030 kA/m (13 kOe). For the $x = 0$ sample, the M_s was 26.9 Am²/kg, and the value increases up to 36.8 Am²/kg with x . Since the structure is that of an inverse spinel and the cations are collinear, the increase of M_s with x can be well explained by the higher magnetic moment of the Co^{2+} ion ($3\mu_{\text{B}}$) compared to that of the Cu^{2+} ion ($1\mu_{\text{B}}$). The coercivity increases from 68.4 kA/m (0.86 kOe) to 175 kA/m (2.2 kOe) when x is increased from 0 to 0.1. Above $x = 0.1$, H_c starts to decline, reaching a value of 71.6 kA/m (0.9 kOe) when $x = 0.2$. In the case of cubic cobalt doped spinel ferrite particles[25]:[26]:[27], coercivity is often almost directly proportional to the Co concentration. This can be attributed to the octahedral Co^{2+} which enhances the magnetocrystalline anisotropy from strong spin orbital coupling[17]:[28]. In this study, the linear relation between coercivity and Co content is broken above $x = 0.1$. Since most of the Cu and Co are in the octahedral sites, the main factor of the magnetic anisotropy is the octahedral Co^{2+} and the variation of coercivity may be due to the added tetragonality factor. The distorted environment by the Cu^{2+} stimulates the magnetoelasticity of the

octahedral Co^{2+} sites, which may be the origin of the higher coercivity in samples with high tetragonality ($x \leq 0.1$), and the lower coercivity in samples with lower tetragonality ($x > 0.1$).

To analyze the intrinsic magnetic anisotropy, we performed rotational hysteresis loss measurements using a torque magnetometer under a maximum applied field of 1.8 T at room temperature. Figure 4 (a) shows the representative inverse magnetic field dependence of the rotational hysteresis loss (W_r) for the $x = 0.1$ sample. With increasing field, W_r showed a peak at 398 kA/m ($H_{\text{app}} = 5$ kOe) and gradually decreases with the applied field. The magnetic anisotropy field H_k is determined by extrapolating the linear part of W_r towards the origin at the high field region[29] and is about 1591 kA/m (20 kOe). Figure 4 (b) shows the relationship between H_k and H_c for the $\text{Cu}_x\text{Co}_{1-x}\text{Fe}_2\text{O}_4$ particles ($x > 0$). For the mixed Cu and Co samples, H_k is linearly proportional to H_c , suggesting that the coercivity is almost a direct measure of the magnetic anisotropy. However, the linear relation is independent of x . This strongly suggests that the magnetic anisotropy does not originate only from the magnetocrystalline anisotropy (K_1) of Co, but also from the tetragonality.

From the anisotropy field, the absolute value of the magnetocrystalline anisotropy constant, $K = \mu_0 M_s H_k / 2$; is estimated to be 0.14 MJ/m^3 for the $x = 0.1$ sample. Dividing this value with $x = 0.1$, we get the magnetic anisotropy constant normalized to CoFe_2O_4 , $K_{\text{Co}} = 1.4 \text{ MJ/m}^3$, which is an order larger than that of the non-strained bulk cubic CoFe_2O_4 ($K_1 = 0.18 - 0.4 \text{ MJ/m}^3$). [30][31] This indicates that the JT distortion in the particles may have affected the local environment of Co ions, rather than exclusively affecting the Cu ions.

The uniaxial strain described as the lattice distortion $\chi(x)$, and the anisotropy sites estimated from the total effective ME coupling coefficient $B_1(x)$ can be expressed as;

$$\chi(x) = -25.1(\pm 5.5)x + 5.34 (\pm 0.67) \quad (1),$$

$$B_1^{\text{tot}}(x) = B_{1\text{Co}}x + B_{1\text{Cu}}(1 - x) \quad (2),$$

where $B_{1\text{Co}}$ and $B_{1\text{Cu}}$ are the ME coefficients per unit Co and Cu ion. Substituting Eq. (1) and (2) in the magnetoelastic model[32][33] $K=B_1\chi$, one gets

$$K_u(x) = (B_{1\text{Co}} - B_{1\text{Cu}})x\chi(x) + B_{1\text{Cu}}\chi(x) \quad (3).$$

Equation (3) simply describes the magnetic anisotropy as a coupling of two independent physical phenomena; which are the tetragonality by the JT effect χ and the magnetoelasticity B_1 . The experimental values of K plotted against $x\chi(x)$ is shown in Figure 5. Solid line represents the linear fit for the tetragonally distorted samples ($\chi > 0$). For $\chi = 0$, the data point of the cubic $x = 0.2$ sample clearly deviated from the other data points, showing the limitation of the magnetoelastic model as tetragonality diminishes.

Using the linear fit obtained by the least-square method, the magnetoelastic coefficients of Co and Cu are determined to be $B_{1\text{Co}} = 40 \text{ MJ/m}^3$ and $B_{1\text{Cu}} = 1.5 \text{ MJ/m}^3$, respectively. The $B_{1\text{Cu}}$ value of bulk Cu ferrite calculated using the reported values of the magnetic anisotropy and tetragonality of bulk Cu ferrite ($K_1 = 0.2 \text{ MJ/m}^3$ [34] and $\chi = 5.6\%$ [19]) is approximately 4 MJ/m^3 . The theoretical $B_{1\text{Co}}$ value for bulk Co ferrites is calculated to be 55 MJ/m^3 using the following B_1 expression for a given cubic lattice with uniaxial distortion

$$B_1 = \frac{3}{2}\lambda_{100}(C_{12} - C_{11}) \quad (4),$$

where the magnetostriction constant ($\lambda_{100} = -250$ [30]) and the respective elastic moduli ($C_{11} = 273$ GPa and $C_{12} = 106$ GPa [35][36]). The calculated $B_{1\text{Cu}}$ and $B_{1\text{Co}}$ values are consistent with our experimental values, suggesting the validity of our proposed magnetoelastic model using the JT effect to explain the magnetic anisotropy of the (Cu,Co)Fe₂O₄ particles.

Conclusions

We have demonstrated the phenomenological model of strain-induced magnetic anisotropy in spinel ferrite particles by the coupling of the JT effect (by Cu²⁺ ions) and the magnetoelastic effect (by Co²⁺ ions). The tetragonal distortion decreases with increasing Co content and the cooperative JT distortion is finally suppressed when $x = 0.2$. The coercivity showed a maximum at $x = 0.1$ and is proportional to the magnetic anisotropy field. The mechanism of magnetic anisotropy is analyzed as follow. For the tetragonally distorted samples in the $x < 0.1$ region, more Co content causes an increase in the anisotropy site, resulting in the increase of the magnetic anisotropy (reflected in the H_c and H_k values). In the $x > 0.1$ region, increasing x suppresses the JT effect and thus reduces the lattice distortion. Eventually, the competition between the lattice strain from Cu²⁺ and the anisotropy site from Co²⁺ contributes to the maximum magnetic anisotropy when $x = 0.1$. This model of strain-induced anisotropy may be applicable to other ferrite systems such as the hexagonal type and open new perspectives in the design and development of permanent magnets and other hard materials.

Acknowledgment

In-field Mössbauer studies were performed at the Tandem Accelerator Complex, University of Tsukuba. This study was supported by the Japan Science and Technology Agency (JST) under Collaborative Research Based on Industrial Demand “High Performance Magnets: Towards Innovative Development of Next Generation Magnets. This work was partly supported by the Grant-in-Aid for Japan Society for the Promotion of Science Research Fellow; JSPS KAKENHI Grant Number JP18J12106. This study was supported by the Laboratoire d’Excellence LANEF in Grenoble (ANR-10-LABX-51-01).

References

- [1] F. K. Lotgering, P. H. G. M. Vromans, and M. A. H. Huyberts, "Permanent-magnet material obtained by sintering the hexagonal ferrite $W = \text{BaFe}_{18}\text{O}_{27}$," *J. Appl. Phys.*, vol. 51, no. 11, pp. 5913–5918, Nov. 1980.
- [2] G. Albanese, M. Carbucicchio, and G. Asti, "Spin-order and magnetic properties of $\text{BaZn}_2\text{Fe}_{16}\text{O}_{27}$ ($\text{Zn}_2\text{-W}$) hexagonal ferrite," *Appl. Phys.*, vol. 11, no. 1, pp. 81–88, Sep. 1976.
- [3] H. Kojima, C. Miyakawa, T. Sato, and K. Goto, "Magnetic properties of W-type hexaferrite powders," *Jpn. J. Appl. Phys.*, vol. 24, no. 1, pp. 51–56, Jan. 1985.
- [4] A. Collomb and J. P. Mignot, "The $\text{Ba}(\text{Sr})\text{Mn}_2\text{Fe}_{16}\text{O}_{27}$ -type hexagonal ferrites as permanent magnets," *J. Magn. Magn. Mater.*, vol. 69, no. 3, pp. 330–336, Nov. 1987.
- [5] A. Lisfi *et al.*, "Reorientation of magnetic anisotropy in epitaxial cobalt ferrite thin films," *Phys. Rev. B*, vol. 76, no. 5, p. 054405, 2007.
- [6] T. Niizeki *et al.*, "Extraordinarily large perpendicular magnetic anisotropy in epitaxially strained cobalt-ferrite $\text{CoFe}_{3-x}\text{O}_4(001)$ ($x = 0.75, 1.0$) thin films," *Appl. Phys. Lett.*, vol. 103, no. 162407, pp. 1–5, 2013.
- [7] J. Inoue, T. Niizeki, H. Yanagihara, H. Itoh, and E. Kita, "Electron theory of perpendicular magnetic anisotropy of Co-ferrite thin films," *AIP Adv.*, vol. 4, no. 027111, pp. 2014–2017, 2014.
- [8] J. Inoue, H. Yanagihara, and E. Kita, "Magnetic anisotropy and magnetostriction in cobaltferrite with lattice deformation," *Mater. Res. Express*, vol. 1, no. 4, p. 046106, Oct. 2015.
- [9] T. Tainosho, J. Inoue, S. Sharmin, and H. Yanagihara, "Large Negative Uniaxial Magnetic Anisotropy of Cobalt Ferrite Thin Films," *Dig. TMRC 2017 28th Magn. Rec. Conf.*, pp. 133–134, 2017.
- [10] B. H. Liu and J. Ding, "Strain-induced high coercivity in CoFe_2O_4 powders," *Appl. Phys. Lett.*, vol. 88, no. 4, pp. 1–3, 2006.
- [11] H. Latiff, M. Kishimoto, S. Sharmin, E. Kita, and H. Yanagihara, "Effect of Copper Substitution on Fe_3O_4 Particles Prepared via Coprecipitation and Flux Methods," *IEEE Trans. Magn.*, vol. 53, no. 1, p. 9400104, 2017.
- [12] H. Latiff, M. Kishimoto, S. Sharmin, E. Kita, H. Yanagihara, and T. Nakagawa, "Enhanced Anisotropy in Tetragonalized $(\text{Cu},\text{Co})\text{Fe}_2\text{O}_4$ Particles via the Jahn–Teller Effect of Cu^{2+} Ions," *IEEE Trans. Magn.*, vol. 53, no. 11, p. 9402304, 2017.
- [13] M. Yokoyama, A. Nakamura, T. Sato, and K. Haneda, "Jahn-Teller Effect in Ultrafine Copper Ferrite Particles," *J. Magn. Soc. Japan*, vol. 22, no. S1, pp. 243–245, 1998.
- [14] P. Tailhades *et al.*, "Cation Migration and Coercivity in Mixed Copper–Cobalt Spinel Ferrite Powders," *J. Solid State Chem.*, vol. 141, no. 1, pp. 56–63, Nov. 1998.

- [15] C. Villette, P. Tailhades, and A. Rousset, "Thermal Behavior and Magnetic Properties of Acicular Copper-Cobalt Ferrite Particles," *J. Solid State Chem.*, vol. 117, no. 1, pp. 64–72, Jun. 1995.
- [16] P. Tailhades, P. Mollaro, A. Rousset, and M. Gougeon, "Structure and Induced Anisotropy of New Cobalt and Manganese Spinel Defect Ferrites," *IEEE Trans. Magn.*, vol. 26, no. 5, pp. 1822–1824, 1990.
- [17] J. C. Slonczewski, "Origin of magnetic anisotropy in cobalt-substituted magnetite," *Phys. Rev.*, vol. 110, no. 6, pp. 1341–1348, 1958.
- [18] R. Skomski and J. M. D. Coey, "Magnetic anisotropy — How much is enough for a permanent magnet?," *Scr. Mater.*, vol. 112, pp. 3–8, Feb. 2016.
- [19] H. Ohnishi and T. Teranishi, "Crystal Distortion in Copper Ferrite-Chromite Series," *J. Phys. Soc. Japan*, vol. 16, no. 1, pp. 35–43, 1961.
- [20] H. Ohnishi, T. Teranishi, and S. Miyahara, "On the Transition Temperature of Copper Ferrite," *J. Phys. Soc. Japan*, vol. 14, no. 1, pp. 106–106, Jan. 1959.
- [21] Z. Klencsár, E. Kuzmann, and A. Vértes, "User-friendly software for Mössbauer spectrum analysis," *J. Radioanal. Nucl. Chem.*, vol. 210, no. 1, pp. 105–118, 1996.
- [22] J. Chappert and R. B. Frankel, "Mössbauer Study of Ferrimagnetic Ordering in Nickel Ferrite and Chromium-Substituted Nickel Ferrite," *Phys. Rev. Lett.*, vol. 19, no. 10, pp. 570–572, Sep. 1967.
- [23] L. Néel, "Antiferromagnetism and ferrimagnetism," *Proc. Phys. Soc. Sect. A*, vol. 65, no. 11, pp. 869–885, Nov. 1952.
- [24] J. S. J. Janicki, J. Pietrzak, A. Porebska, "Mossbauer study of copper ferrite," *Phys. Status Solidi*, vol. 95, pp. 95–98, 1982.
- [25] A. Malats i Riera, G. Pourroy, and P. Poix, "High coercivity of a cobalt doped magnetite Fe_{2.38}Co_{0.62}O₄," *J. Magn. Magn. Mater.*, vol. 134, no. 1, pp. 195–198, May 1994.
- [26] V. K. Chakradhary, A. Ansari, and M. J. Akhtar, "Design, synthesis, and testing of high coercivity cobalt doped nickel ferrite nanoparticles for magnetic applications," *J. Magn. Magn. Mater.*, vol. 469, pp. 674–680, Jan. 2019.
- [27] D. H. Han, J. P. Wang, and H. L. Luo, "The induced effective uniaxial anisotropy of Mn and Co volume-doped acicular γ -Fe₂O₃ particles," *J. Magn. Magn. Mater.*, vol. 145, no. 1–2, pp. 199–204, Mar. 1995.
- [28] M. Tachiki, "Origin of the Magnetic Anisotropy Energy of Cobalt Ferrite," *Prog. Theor. Phys.*, vol. 23, no. 6, pp. 1055–1072, 1960.
- [29] I. S. Jacobs and F. E. Luborsky, "Magnetic anisotropy and rotational hysteresis in elongated fine-particle magnets," *J. Appl. Phys.*, vol. 28, no. 4, pp. 467–473, 1957.

- [30] R. M. Bozorth, E. F. Tilden, and A. J. Williams, "Anisotropy and magnetostriction of some ferrites," *Phys. Rev.*, vol. 99, no. 6, pp. 1788–1798, 1955.
- [31] H. Shenker, "Magnetic anisotropy of cobalt ferrite ($\text{Co}_{1.01}\text{Fe}_{2.00}\text{O}_{3.62}$) and nickel cobalt ferrite ($\text{Ni}_{0.72}\text{Fe}_{0.20}\text{Co}_{0.08}\text{Fe}_2\text{O}_4$)," *Phys. Rev.*, vol. 107, no. 5, pp. 1246–1249, 1957.
- [32] B. Schulz and K. Baberschke, "Crossover from in-plane to perpendicular magnetization in ultrathin Ni/Cu(001) films," *Phys. Rev. B*, vol. 50, no. 18, p. 13 467-13 471, 1994.
- [33] R. Thamankar, A. Ostroukhova, and F. O. Schumann, "Spin-reorientation transition in $\text{Fe}_x\text{Ni}_{1-x}$ alloy films," *Phys. Rev. B*, vol. 66, no. 13, pp. 1344141–1344148, 2002.
- [34] N. T. Malafaev, A. A. Murakhovskii, J. A. Popkov, and I. Onyszkiewicz, "A study on magnetocrystalline anisotropy in tetragonal copper ferrite," *J. Magn. Magn. Mater.*, vol. 89, no. 1–2, pp. 8–12, 1990.
- [35] M. D. Sturge, E. M. Gyorgy, R. C. Lecraw, and J. P. Remeika, "Magnetic behavior of cobalt in garnets. II. Magnetocrystalline anisotropy and ferrimagnetic resonance of cobalt-doped yttrium iron garnet," *Phys. Rev.*, vol. 180, no. 2, pp. 413–423, Apr. 1969.
- [36] Y. Suzuki, G. Hu, R. B. B. van Dover, and R. J. J. Cava, "Magnetic anisotropy of epitaxial cobalt ferrite thin films," *J. Magn. Magn. Mater.*, vol. 191, no. 1–2, pp. 1–8, Jan. 1999.

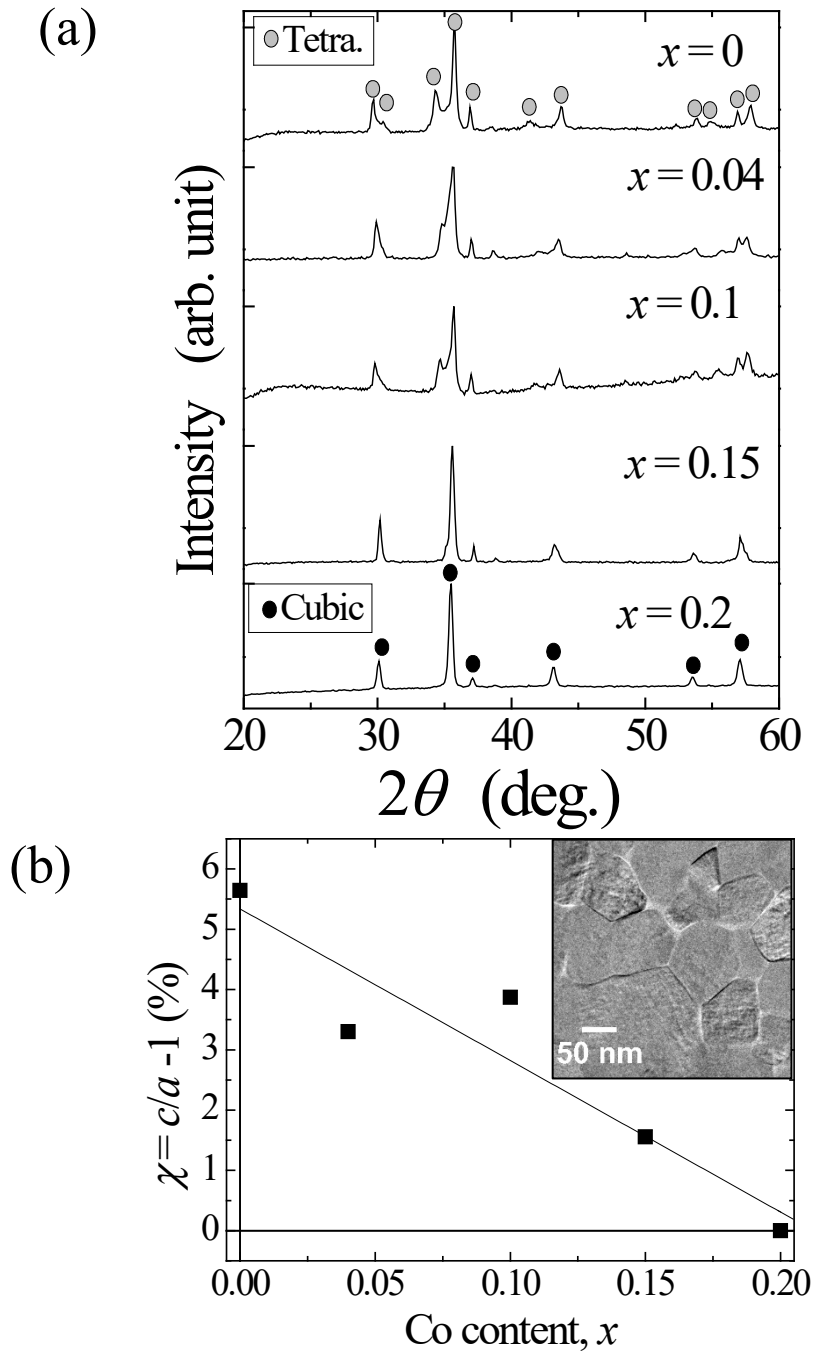


FIG. 1 (a) XRD patterns of the $\text{Cu}_{1-x}\text{Co}_x\text{Fe}_2\text{O}_4$ particles. Black markers represent the peaks attributed to the cubic spinel phase whereas grey markers represent that to the tetragonal spinel phase. (b) Tetragonality χ shows a decreasing tendency due to the suppression of JT effect with increasing Co content. TEM image of the tetragonal $x = 0.1$ sample reveals spherical-like particles with no shape anisotropy (inset).

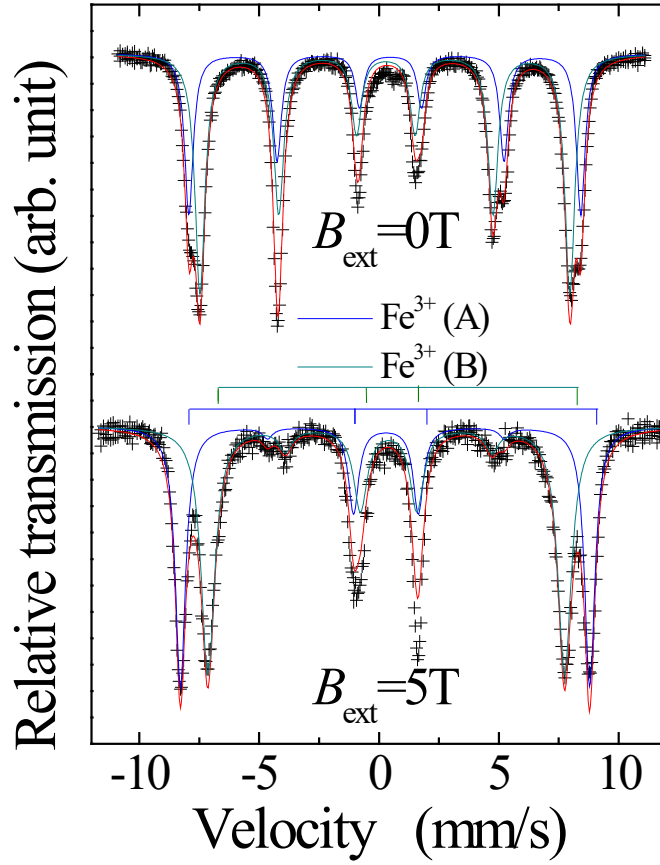


FIG. 2 Room temperature ^{57}Fe Mössbauer spectra of the tetragonal $\text{Cu}_{1-x}\text{Co}_x\text{Fe}_2\text{O}_4$ ($x=0.1$) sample without external magnetic field (top) and with 5T external magnetic field applied along the propagation of the γ -ray (bottom). Solid lines show the results of the fit (see Table 1).

TABLE I Mössbauer parameters: hyperfine field (B_{hf}), isomer shift ($I.S.$), quadrupole split ($Q.S.$), and Fe^{3+} area population (%) for the tetragonal $\text{Cu}_{1-x}\text{Co}_x\text{Fe}_2\text{O}_4$ ($x=0.1$) particles at room temperature.

B_{ext} (T)	Line spectrum	B_{hf} ± 0.03 (T)	$I.S.$ ^a ± 0.01 (mm/s)	$Q.S.$ ± 0.01 (mm/s)	$L.W.$ ± 0.01 (mm/s)	Area (%)
0	Fe^{3+} (A)	47.99	0.27	-0.04	0.502	63.3
	Fe^{3+} (B)	50.84	0.36	-0.24	0.433	36.7
5	Fe^{3+} (A)	53.10	0.27	-0.04	0.517	43.4
	Fe^{3+} (B)	46.27	0.35	-0.10	0.686	56.7

^a Relative to room temperature α -Fe

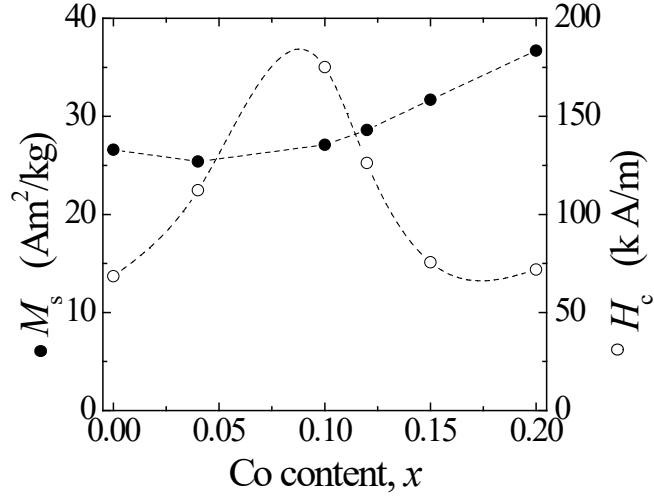


FIG. 3 Room temperature saturation magnetization, M_s (closed-circles) and coercivity, H_c (opened-circles) of $\text{Cu}_{1-x}\text{Co}_x\text{Fe}_2\text{O}_4$ particles ($H_{\text{max}}=1030$ kA/m).

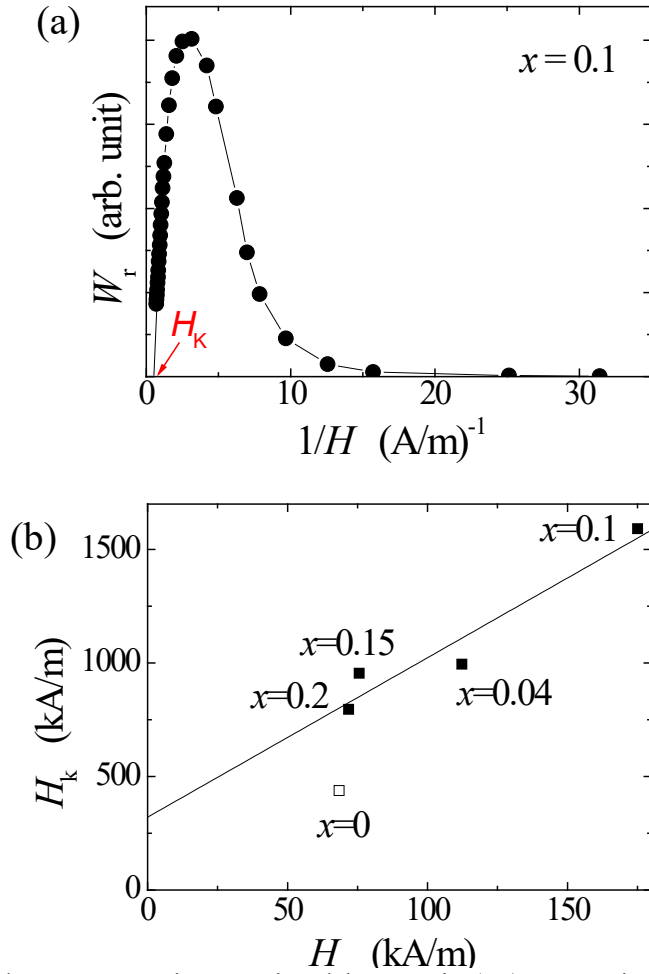


FIG. 4 (a) The representative rotational hysteresis (W_r) versus inverse applied field ($1/H$) plot. (b) Anisotropy field vs. coercivity plot showed a linear relation for $x > 0$ samples (closed-squares), suggesting that the coercivities are almost a direct measure of the magnetic anisotropies in this region.

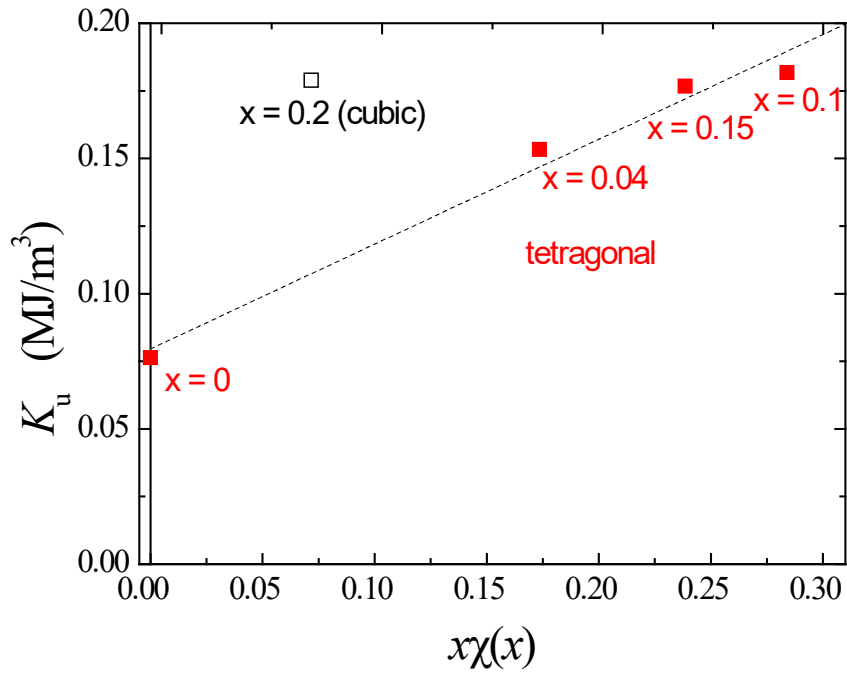


FIG. 5 Plot of the experimental K versus $x\chi$, to model the JT distortion and ME coupling. Closed squares represent tetragonally distorted ($0 < x \leq 0.1$) samples, whereas the opened square is the cubic $x = 0.2$ sample.